Suplemento de la Revista Mexicana de Física **3** 0308121 (2022) 1–4

Chiral condensates for neutron stars in hadron-quark crossover; from a parity doublet nucleon model to an NJL quark model

T. Minamikawa

Department of Physics, Nagoya University, Nagoya 464-8602, Japan.

T. Kojo

Key Laboratory of Quark and Lepton Physics (MOE) and Institute of Particle Physics, Central China Normal University, Wuhan 430079, China.

M. Harada

Department of Physics, Nagoya University, Nagoya 464-8602, Japan.
Kobayashi-Maskawa Institute for the Origin of Particles and the Universe, Nagoya University, Nagoya 464-8602, Japan.
Advanced Science Research Center, Japan Atomic Energy Agency, Tokai 319-1195, Japan.

Received 15 January 2022; accepted 11 May 2022

In this contribution, we summarize our recent studies on the chiral invariant mass and the chiral condensates in neutron star matter. We construct a unified equations of state assuming the crossover phase transition from hadronic matter described by a parity doublet model to quark matter by an Nambu–Jona-Lasinio type quark model. We first show that the chiral invariant mass is constrained to be $600\,\mathrm{MeV} \lesssim m_0 \lesssim 900\,\mathrm{MeV}$ from recent observations of neutron stars. We then determine the density dependence of the chiral condensate in the crossover description, and show that the chiral condensates are actually smoothly connected from the hadronic matter where the change is driven by the positive chiral scalar charge in a nucleon, to the quark matter where the change is by the modification of the quark Dirac sea, reflecting the hadron-quark crossover.

Keywords: Chiral symmetry; chiral condensate; parity doublet model; high density nuclear matter; neutron star.

DOI: https://doi.org/10.31349/SuplRevMexFis.3.0308121

1. Introduction[i]

Chiral symmetry is a symmetry of quantum chromodynamics (QCD) which plays an important role in the hadron dynamics at low energy. In vacuum the chiral symmetry is spontaneously broken by the condensation of quark-antiquark pairs, called chiral condensate σ. The change of vacuum structure produces the quark mass gap of ~ 300 MeV. In high energy region, such as in high temperature or in high density environment, the chiral symmetry is restored with vanishing σ. In a class of effective models, the majority of the nucleon mass comes from the chiral condensate. On the other hand, the lattice simulation in Ref. [3] shows that the nucleon mass remains large even at a temperature with substantial reduction of σ. One of the effective models which reflect this property is the parity doublet model [4, 5] in which nucleons have substantial chiral invariant masses.

One of laboratories to study the roles of the chiral symmetry is a neutron star in which a matter at supra nuclear densities are realized. The density of a neutron star reaches baryon densities (n_B) several times greater than the nuclear saturation density $n_0 \approx 0.16\,\mathrm{fm}^{-3}$, and may accommodate quark matter at the core. The transition from hadronic to quark matter, which is supposed to occur in neutron stars, should give us insight into the nature of chiral symmetry breaking and its restoration.

One of the key observables in neutron star physics is mass-radius sequence of neutron stars (M-R relation), which has a one-to-one correspondence with the underlying equation of state (EOS). The shape of the M-R curve is correlated with the stiffness of EOS at several fiducial densities [6]. The low density part ($n_B \lesssim 2n_0$) is largely correlated with the overall radii of neutron stars while the high density part ($n_B \gtrsim$ 3-5n_0) determines the maximum mass. The neutron star observations and nuclear physics suggest EOS should be soft enough to pass the constraints from the tidal deformability in GW170817 event, $R_{1.4} \lesssim 13$ km for $1.4M_\odot$ neutron star. Meanwhile the heaviest neutron star currently known is PSR J0740+6620 with the mass $2.08 \pm 0.07M_\odot$ and the radius $\simeq 12.4 \pm 0.7$ km, requiring EOS to be very stiff at high density. This soft-to-stiff combination disfavors radical softening and strong first order phase transitions for $\sim$ 2-5n_0. This leads us to the hadron-quark continuity picture as a baseline to describe EOS from hadronic to quark matter. The possible weak first order phase transitions may be treated as perturbations. In practice we consider the 3-window modeling [7]: we use a parity doublet model (PDM) for $n_B \leq 2n_0$, a Nambu–Jona-Lasinio (NJL) type quark model for $n_B \geq 5n_0$, and interpolate them to describe EOS at 2-5n_0. Our interpolation is highly constrained by neutron star observables and the causality condition with the sound velocity less than the light velocity.

The comparison of our M-R relations with observations give us the estimates on the range of our model parameters and microscopic insights into the dynamics. Actually, one can proceed further by extending the interpolation from physical EOS, $P(\mu_B)$, to a general generating function, $P(\mu_B; \mathbf{J})$, in which external sources $\mathbf{J}$ are coupled to various condensates and flavor densities. After constructing a unified functional with various sources, one can differentiate the functional with $\mathbf{J}$ to compute various quantities such as chiral and diquark condensates as well as flavor compositions [2]. This updates the 3-window modeling from thermodynamic quantities to more microscopic quantities which are not directly measured but are important to characterize the state of matter in dense QCD.

2. Models

In this section, we explain a PDM for hadronic matter and an NJL model for quark matter.

2.1. Parity doublet model for hadronic matter

A PDM contains two iso-doublets of nucleon fields $\psi_{1,2}$ to describe positive and negative parity nucleons. The fields ψ_1 and ψ_2 acquire the opposite phases under chiral transformations,

$$\psi_{1L} \to g_L \psi_{1L}\,, \quad \psi_{1R} \to g_R \psi_{1R}\,, \tag{1}$$

$$\psi_{2L} \to g_R \psi_{2L}\,, \quad \psi_{2R} \to g_L \psi_{2R}\,, \tag{2}$$

where g_L and g_R are elements of SU(2)$_L$ and SU(2)$_R$ chiral groups respectively, and left-handed and right-handed fields are defined as

$$\psi_{iL} = \frac{1-\gamma_5}{2}\psi_i\,, \quad \psi_{iR} = \frac{1+\gamma_5}{2}\psi_i\,, \tag{3}$$

for $i = 1, 2$.

Such assignment of the chirality is called mirror assignment. With these fields, one can construct terms including a chiral invariant mass m_0, as

$$m_0(\bar{\psi}_1\gamma_5\psi_2 + h.c.)\,. \tag{4}$$

There are also Yukawa terms as in ordinary linear sigma models, $g_1\bar{\psi}_1\sigma\psi_1$ and $g_2\bar{\psi}_2\sigma\psi_2$. The effective potential of σ field is minimized for a non-zero σ, which produces the chiral variant mass for nucleons. The diagonalization of chiral invariant and variant components leads to the mass spectra

$$m_{N,N^*} = \sqrt{m_0^2 + G_+^2\sigma^2} \mp G_-\sigma \tag{5}$$

where $G_\pm = |g_1 \pm g_2|/2$. For vanishing chiral condensate, the nucleon remains massive; $m_N(m_{N^*}) \to m_0$ as $\sigma \to 0$. We note that, for larger m_0, the mass of nucleon is dominated by the chiral invariant mass m_0 so that $G_\pm$ should be smaller. Namely, the nucleon fields $\psi_{1,2}$ couples to σ field weakly for a large m_0.

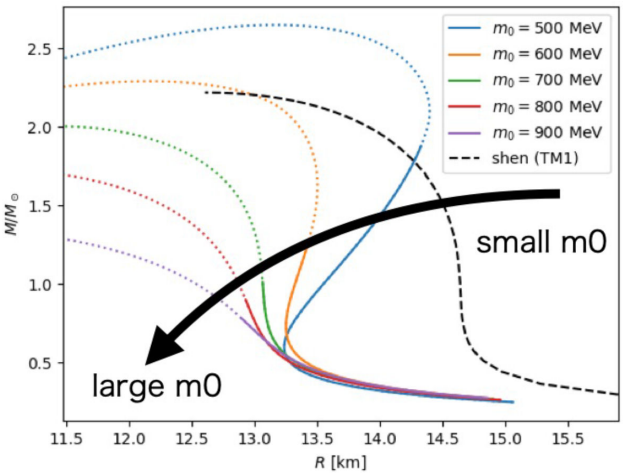

FIGURE 1. $M-R$ relations obtained from the PDM for $m_0 = 500$, 600, 700, 800, and 900 MeV. The solid curves show the M-R relations for $n_c < 2n_0$, where n_c is the central density.

For descriptions of hadronic matter, in addition we include ω and ρ meson fields, which are necessary to reproduce the nuclear saturation properties at $n_B = n_0$ and the symmetry energy. For symmetric nuclear matter, the attractive contribution from σ field and repulsive contribution from ω field are balanced. We were able to tune parameters to reproduce the saturation properties, but the high density extrapolation is very sensitive to the values of m_0. For large m_0, the N-σ coupling is weak. Then, the N-ω coupling needed to reproduce the saturation properties is small enough to be balanced with the σ attraction. As density exceeds n_0, weaker ω repulsion leads to softer EOS and smaller radius of neutron star. The trend is opposite for a small m_0. The trend can be seen in Fig. 1.

2.2. NJL model for quark matter

For quark matter we use the standard three-flavor NJL model with additional two terms: the interaction leading to the diquark condensates $H(q^t\Gamma_a q)(\bar{q}\Gamma^a\bar{q}^t)$ and the vector-type interaction $g_V(\bar{q}\gamma^\mu q)^2$. We explore the range of the coupling constants (g_V, H) which are consistent with neutron star observations and the causality condition.

2.3. Unified EOS with interpolation

To construct a unified EOS, the EOSs of the PDM and the NJL model are interpolated with the following polynomial

$$P_{\rm Interp} = \sum_{i=0}^{5} a_i \mu_B^i\,. \tag{6}$$

The six coefficients $a_0, \cdots, a_5$ are determined by matching the polynomial with hadronic and quark EOS at the boundaries up to the second orders in derivatives. The hadronic and quark boundaries are $n_B = 2n_0$ and $5n_0$, respectively. The EOSs satisfying the causality condition $c_s^2 = dP/d\varepsilon \le 1$ can be adopted as physical EOSs.

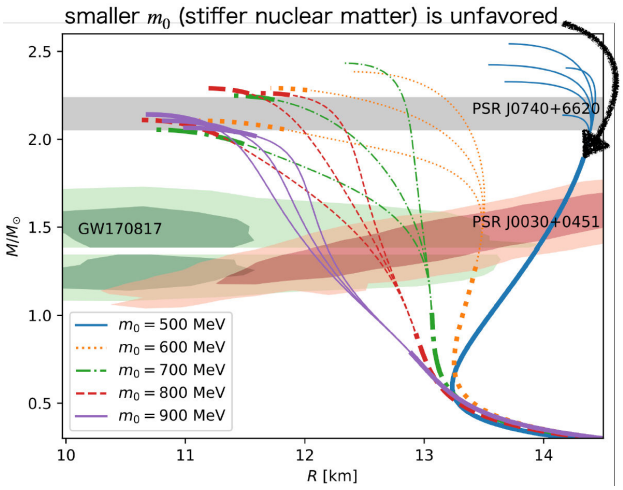

FIGURE 2. M-R relations calculated from the unified EOSs. The solid blue curves pointed by the arrow are for $m_0 = 500$ MeV.

3. Results

3.1. M-R relation

Shown in Fig. 2 are some selected results of M-R relations for unified EOSs for various m_0 [1]. For neutron stars with the mass $\lesssim 0.5M_\odot$, the curves for different m_0 show roughly the same behavior. The bold parts of the curves correspond to EOS at $n_B \leq 2n_0$, from which one can see that the overall radii of neutron stars are largely determined by hadronic EOS.

We note that, in Fig. 2, we show M-R curves for which the maximum masses exceed the highest mass of the observed neutron star. The solid blue curves pointed by the arrow are for $m_0 = 500\,\mathrm{MeV}$, which correspond to the stiffest hadronic matter in our model. The radii are too large to be compatible with the constraints from GW170817 (the green shades). Therefore, we omit the m_0 case and conclude that the favored range of m_0 is

$$600\,\mathrm{MeV} \lesssim m_0 \lesssim 900\ \ \mathrm{MeV}\,. \tag{7}$$

That implies that the large portion of the nucleon mass comes from the chiral invariant mass, and the N-σ and N-ω couplings are weaker than the conventional linear σ model with $m_0 = 0$.

3.2. Chiral condensate

Our interpolation procedures for thermodynamic potentials can be extended to generating functionals with external sources $\mathbf{J}$. We can estimate condensates coupled to $\mathbf{J}$ by taking the derivatives of the thermodynamic potential with respect to $\mathbf{J}$. One example is the chiral condensate. Treating the current quark masses as external sources, one can use the Hellmann-Feynman theorem to calculate the chiral condensates

$$\langle \bar{q}q \rangle = \frac{\partial \Omega}{\partial m_q}\,. \tag{8}$$

In practice, we construct the generating functionals for hadronic and quark matter and calculate the corresponding boundary conditions at $2n_0$ and $5n_0$. These boundary conditions constrain the possible functionals in the interpolation region. In this way, the condensates in the interpolated domain capture the trends of both hadronic and quark matter.

In the PDM, the trend of the chiral restoration is similar to what we infer from the linear density approximation which should be valid in dilute regime. The key observation is that nucleons carry the positive chiral scalar charges whose signs are opposite to the negative vacuum scalar density. Hence increasing baryon density neutralizes the chiral scalar density σ. Meanwhile, the extrapolation of this picture toward high baryon density eventually leads to the system with full of positive scalar charges, see Fig. 3 for the flip of the sign in σ. This seems odd with quark model predictions in which chiral condensates lose the magnitudes at high density; for instance, the NJL model predicts that the in-medium chiral condensates are about 20% of the vacuum counterparts. For the interpolated domain, these trends of hadronic and quark model descriptions are balanced by matching the interpolating functions with the hadronic and quark matter boundaries. Figure 3 is the ratio of the obtained chiral condensates to the vacuum values for various choices of m_0 and (g_V, H). For comparison, we also show the extrapolation of the PDM and linear density approximation beyond the hadronic domain. We note that, while the PDM shows wild variations for different values of m_0 for the domain $n_B = 2$-$5n_0$, our unified modeling tempers the m_0 dependence by putting quark model constraints from the high density side.

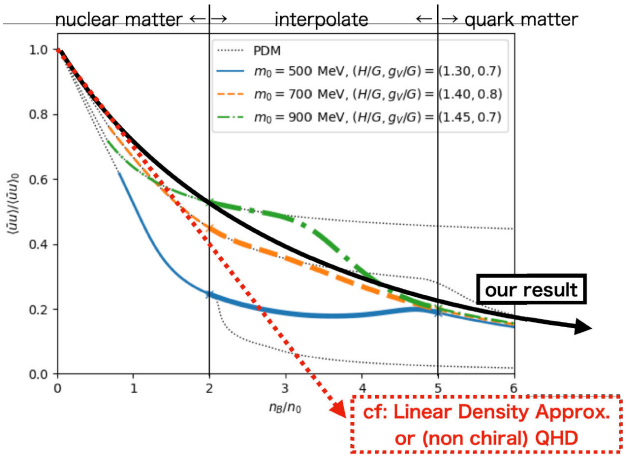

FIGURE 3. Ratio of the obtained chiral condensates to the vacuum values vs. the baryon number density. All curves of our results remain positive and approach to zero gradually, as indicated by solid black arrow. On the other hand, the typical results obtained from *e.g.*, linear density approximation or non-chiral QHD flip their signs at some high density as indicated by dotted red arrow.

In qualitative terms, the hadronic and quark models are supposed to cover the different aspects of the chiral restoration. In typical hadronic models, one does not manifestly consider the structural changes of nucleons around n_0. Nevertheless the chiral restoration can take place simply due to the scalar charges inherent to nucleons. In this picture, the reduction of spatial average of the vacuum and nucleon scalar densities does not immediately mean the significant reduction of the magnitude in vacuum and in nucleons for each. With this description, the dynamical mass, *e.g.*, constituent quark masses in a nucleon can remain large even after σ is reduced by $\sim 30\%$ at n_0 and $\sim$ 40-80% at $2n_0$ as predicted by the PDM. In the PDM, the chiral invariant mass m_0 plays the role to keep nucleons massive in hadronic domain. In contrast, the quark models deal with the reduction of chiral condensates in magnitude not at the level of spatial average but at each location. For instance the NJL model predicts the modification of the quark Dirac sea and associated reduction of the constituent quark masses. In terms of the chiral invariant mass m_0, the quark models at high density predict the reduction of m_0. Our interpolation balances these different chiral restoration in a somewhat balanced way.

4. Summary and discussion

Firstly, we showed that the PDM with the substantial chiral invariant mass, $600\,\mathrm{MeV} \lesssim m_0 \lesssim 900\,\mathrm{MeV}$, can provide M-R relation of neutron stars consistently the observations. In the future, the further observations of neutron stars may restrict the chiral invariant mass more strictly, because the typical radius of a neutron star (with *e.g.* $M \approx 1.4 M_\odot$) is strongly correlated with the property of the hadronic matter. Moreover, since the model parameters of hadronic and quark matter constrain each other through the thermodynamically consistent interpolation, the parameters of the NJL model can also be restricted at the same time.

Second, we showed that the chiral condensate in the hadronic matter where the change of the chiral condensate is driven by the scalar density of baryons, is smoothly connected to the one in the quark matter where the change is by the modification of quark Dirac sea. PDM reflects the property that the nucleon mass does not change much, and this property is consistent with ignoring the density dependence of Dirac sea in the hadronic matter. On the other hand, Dirac sea plays an important role in the NJL model. It can be said that our crossover description connects the property of the hadronic matter and the change of the vacuum structure in the quark matter smoothly. This is one of the results that reflect the hadron-quark crossover picture.

Here, let us discuss the inhomogeneous chiral condensates qualitatively. A naive extrapolation of the linear density approximation indicates that the scalar charge of a nucleon almost cancels the chiral condensate in vacuum, so that the chiral condensate in a nucleon may have the opposite sign to the vacuum one. Therefore, when the baryon density increases, the space average of the chiral condensate can flip its sign. However, according to our result, the chiral condensate keeps its sign and approaches zero gradually. If the chiral condensate has a wave form in the sufficiently high density medium, the space average can vanish.

In this work, we assumed that the hyperons do not contribute in the lower density $n_B < 2n_0$. If one extend the PDM to a three-flavor model and adopt its EOS up to even higher density e.g. $n_B < 3n_0$, we can discuss the behavior of the strange quark contribution in neutron star more precisely.

Acknowledgments

The work of T.M. and M.H. was supported in part by JSPS KAKENHI Grant No. 20K03927. T.M. was also supported in part by the Department of Physics, Nagoya University. T.K. was supported by NSFC Grant No. 11875144.

---

i. This talk is mainly based on our papers of Refs. [1, 2].

1. T. Minamikawa, T. Kojo and M. Harada, Quark-hadron crossover equations of state for neutron stars: constraining the chiral invariant mass in a parity doublet model, *Phys. Rev. C* **103** (2021) 045205, https://doi.org/10.1103/PhysRevC.103.045205.
2. T. Minamikawa, T. Kojo and M. Harada, Chiral condensates for neutron stars in hadron-quark crossover: From a parity doublet nucleon model to a Nambu–Jona-Lasinio quark model, *Phys. Rev. C* **104** (2021) 065201, https://doi.org/10.1103/PhysRevC.104.065201.
3. G. Aarts, C. Allton, D. De Boni, S. Hands, B. Jäger, C. Praki and J. I. Skullerud, Light baryons below and above the deconfinement transition: medium effects and parity doubling, *JHEP* **06** (2017) 034, https://doi.org/10.1007/JHEP06(2017)034.
4. C. E. Detar and T. Kunihiro, Linear σ Model With Parity Doubling, *Phys. Rev. D* **39** (1989) 2805, https://doi.org/10.1103/PhysRevD.39.2805.
5. D. Jido, M. Oka and A. Hosaka, Chiral symmetry of baryons, *Prog. Theor. Phys.* **106** (2001) 873-908, https://doi.org/10.1143/PTP.106.873.
6. T. Kojo, Delineating the properties of matter in cold, dense QCD, *AIP Conf. Proc.* **2127** (2019) 020023, https://doi.org/10.1063/1.5117813.
7. G. Baym, T. Hatsuda, T. Kojo, P. D. Powell, Y. Song and T. Takatsuka, From hadrons to quarks in neutron stars: a review, *Rept. Prog. Phys.* **81** (2018) 056902, https://doi.org/10.1088/1361-6633/aaae14.